



DELIVERABLE 4.1.

“Numerical Simulations of the Stress Release Process under Deep Drilling Conditions”

ABSTRACT

The objective of the work defined in WP4.1 is to numerically simulate the effect of the geometry of the bottom-hole and the effect of the presence of a groove as well as its depth on the evolution of the stress state at the bottom-hole in a zone very close to the action of the drilling bit on the rock. The drilling action itself is not considered in these first quasi-static numerical simulations.

Given the high strength of the granites studied, the simulations were carried out mainly within the framework of an axisymmetric elastic model for three bottom-hole profiles: flat, convex and concave. These profiles were found to be key factors that can be played on to optimize the stress relaxation process. With a concave profile, the rock relaxation process is more important (reduction of the mean stress and deviator) and this even in the absence of a peripheral groove.

The results indicate that the presence of a peripheral groove can induce a reduction of more than 50% of the mean stress in the immediate vicinity of the drilling bit action provided that the depth of the groove reaches 20 to 30% of the hole radius.

An optimal combination of the drilling bit profile and groove geometry is therefore possible to reduce the mean stress at the bottom-hole and thus hope to reduce the resistance of the rock to the action of the drilling bit in order to improve the ROP. This optimization work will be conducted in WP4.3.

Furthermore, simulations show that, under the same initial stress regime, the evolution of the stress state during laboratory tests on Armines vertical drilling bench using full scale drilling bits (planned in WP4.2) is very close to that obtained at the scale of a real drilling. A test protocol is proposed to make the test as representative as possible of the reality of deep drilling.

Disclaimer

The present document reflects only the author’s view. The European Innovation and Networks Executive Agency (INEA) is not responsible for any use that may be made of the information it contains.

DOCUMENT TYPE:	Deliverable
DOCUMENT NAME:	Numerical simulations of the stress release process under deep drilling conditions
VERSION:	vfinal
DATE:	09/10/2021
STATUS:	S0
DISSEMINATION LEVEL:	PU

AUTHORS, REVIEWERS			
AUTHOR(S):	Hedi SELLAMI, Emad JAHANGIR		
AFFILIATION(S):	ARMINES/ Mines ParisTech		
FURTHER AUTHORS:			
PEER REVIEWERS:	Florian CAZENAVE (Drillstar), John-Paul LATHAM assisted by Sadjad NADERI (ICL), Laurent GERBAUD, Naveen VELMURUGAN (ARMINES)		
REVIEW APPROVAL:	Approved	Yes	Rejected (to be improved as indicated below)
REMARKS / IMPROVEMENTS:	<p>Florian CAZENAVE : Very interesting study</p> <p>John-Paul LATHAM : The groove and or shape effect is shown to have dramatic effect on the elastic stress state. Many comments have been included for consideration but there is a limit to how far one can go with the elastic approach. It will become all the more interesting when some drill loadings perturb these elastic states of stress to confirm extra rock vulnerability with the grooves or concave geometries.</p> <p>Authors' response : This report deals with the effect of the bottom hole profile and the depth of the groove on the change of the stress state in the immediate vicinity of the future bit action, without considering at this stage the mechanical action of the bit. In order to specify the optimal geometry of the groove and the best profile of the drill bit, numerical simulations combining these stress states and the loading action of the drill bit will be performed in WP4.3, while considering the most appropriate rock failure criterion.</p>		

VERSION HISTORY			
VERSION:	DATE:	COMMENTS, CHANGES, STATUS:	PERSON(S) / ORGANISATION SHORT NAME:
v0.1	21/09/21	First draft from ARMINES	Hedi (Armines)
v1.1	23/09/21	First peer reviewer	Florian (Drillstar)
v1.2	26/09/21	Second peer reviewer	JP (ICL)
v2.1	06/10/21	Second review from peer reviewer	JP (ICL)
VFINAL	08/10/21	Final version with all reviews included	Hedi (ARMINES)

VERSION NUMBERING	
v0.x	draft before peer-review approval
v1.x	After the first review
v2.x	After the second review
vfinal	Deliverable ready to be submitted!

STATUS / DISSEMINATION LEVEL			
STATUS		DISSEMINATION LEVEL	
S0	Approved/Released/Ready to be submitted	PU	Public
S1	Reviewed	CO	Confidential, restricted under conditions set out in the Grant Agreement
S2	Pending for review		
S3	Draft for comments	CI	Classified, information as referred to in Commission Decision 2001/844/EC.
S4	Under preparation		

TABLE OF CONTENTS

1	Reminder of WP4 objectives	4
2	Numerical assessment of stress concentration on the bottom-hole	5
2.1	Introduction	5
2.2	Stress concentration	6
2.3	How to release stress concentration	7
3	Optimization of the stress release process	9
3.1	Effect of groove depth	9
3.2	Failure criteria	10
4	Can these processes be reproduced under laboratory conditions	15
5	General conclusions	16
6	Discussions and perspectives	17
6.1	Initial stress state and limit of axisymmetric simulations	17
6.2	Thermal effect	18
7	References	19

CONTENT

1 Reminder of WP4 objectives

The starting point of ORCHYD project is that deep rocks are subject to high down-hole stresses, which make the rock more resistant, reducing the efficiency of the mechanical action of the drilling bit.

To address this problem, which is responsible for the downfall of the deep penetration rate (ROP), key questions can be asked:

- How does stress concentrate at the bottom-hole in the immediate vicinity of the drilling bit?
- Can these stresses be released and how this can be achieved?
- How effective is to modify the bottom-hole profile?
- How effective is to create new free surface, by slotting groove at the drilling face?
- Finally, if these solutions are effective, can we then control and maximise the process of stress release of the rock in the immediate vicinity of the drilling bit action?

Reflection on these points defines the two main objectives of this **WP4** :

1. Reproduce and demonstrate, using both numerical modelling and drilling tests, the impact of Stress Release Process on increasing drilling performance when the rock is subject to pressure up to 100 MPa and temperature up to 200°C
2. Provide the best down-hole configurations in terms of bottom-hole profile and optimal peripheral groove configurations, enabling to improve by a factor of 3 the ROP, when using the best adapted drilling bit.

According to these objectives, the work was organised as follows:

A first task is devoted to the numerical simulations in order to :

- Built relevant numerical mechanical model able to reproduce stress distribution around a deep hole using relevant rock behaviour laws, including failure criteria
- Quantify the stress concentration phenomena around the bottom-hole under various down-hole conditions
- Specify the redistribution of the stresses and their magnitude around peripheral grooves created on the drilling face
- Provide, for a given depth and hole diameter, the ideal drilling face profile in terms of : bottom-hole profile, depth of the groove to be slotted (using HPWJ, WP5). The ideal configuration is the one that allows the maximum weakening of the rock at the immediate vicinity of the drilling bit action.

The final objective of these simulations is to provide a preliminary design of the ideal geometry of the grooves to be slotted.

A second task provides a proof-of-concept demonstration of the benefit of the self-release stress on ROP. This involves the following steps:

- demonstrate the expected penalizing effect of the high pressure regime at the bottom-hole
- validate, using laboratory drilling tests in realistic conditions, the expected positive effect of releasing the stresses while drilling in hard rocks

This should be done using the three major commercial families of drilling bits: PDC bit which exhibit a shear cutting process, the roller cone bit which exhibit a quasi-static indentation process and the rotary hammer bit which exhibit a dynamic process. In ORCHYD, it is expected a higher effect when using percussive hammer bit, which is why the project was oriented towards this solution.

Finally, a third task exploits the lessons learned from tasks 1 and 2, as well from WP5 which is dedicated to optimise the kerfing action of HPWJ in hard rocks under high down-hole pressure regime. Numerical simulations will be conducted in order to assess the validity of the previous results and to confirm the validity of the initial designs in terms of grooves design and bit profile. These designs are needed for **WP7** dedicated to design and manufacture prototypes of HPWJ assisted percussive rotary drilling bits.

This report summarizes the work undertaken in Task 1 presented above.

2 Numerical assessment of stress concentration on the bottom-hole

2.1 Introduction

The literature review shows a large number of studies on cutting and coring process in deep rocks. In this framework, the main purpose of stress analyses is often to explain some phenomena such as borehole instability and failure or core diskings (Bahrani et al, 2015). The state of stress regimes in highly stressed deep rocks as well as the process of stress release, to our knowledge, not been studied when applied to the drilling mechanism in order to improve ROP.

Within the framework of task1 of ORCHYD WP4, numerical simulations have been performed using Abaqus Software mainly under axisymmetric condition. The target depth of the project is located between 4 and 6 km, where the geological formations are mainly constituted of hard crystalline rock, granites in particular. Considering the high stiffness of these rocks and following the results of the first simulations carried out, it was thought more appropriate to use first an elastic behaviour law and compare the resulted stress states with different, commonly used, failure criteria in rock mechanics via a post-processing process.

Based on the material parameters deduced from classical tri-axial tests, the groove creation process will not lead to an exceedance of the failure criterion of the studied rock, which justified the use of an elastic simulation in a first step with post-processing verification of the stress

state. Naturally, when the loading due to the action of the drilling bit is taken into account, a model taking into account the failure process will be required.

Table 1 shows the characteristics of the studied granite. These parameters were obtained on undisturbed laboratory macroscopic scale samples.

Table 1. Mechanical parameters of the studied granite.

Density (kg/m ³)	Sound velocity (m/sec)	UTS (MPa)	UCS (MPa)	Cohesion (MPa)	Ø° (friction angle)	Young Modulus (GPa)	Poisson Coeff.
2635	5600	8	150	25	58	60	0.25

The results presented below correspond to the case of 4 km drilling depth, described by an initial horizontal and vertical stress state $s_h=s_v=-100$ MPa and a -40 MPa applied drilling mud pressure. The drilled hole diameter is 20 cm and the groove width is 5 mm. Three bottom-hole profiles are considered: flat, convex, and concave.

2.2 Stress concentration

To quantify stress concentration around the bottom-hole we need to introduce a relevant parameter. We present here the normalized radial stress (s_r/s_{r0}) and normalized mean stress (p/p_0) that we believe could be appropriate candidates to sum up the stress concentration factor. The zero index stands for the rock initial state before drilling the hole, the stress concentration appears when stress ratios are greater than 1. Figures 1 and 2 show the distribution of the stress concentration factor for the mean stress and radial stress.

The radial stress concentration factor seems be more sensitive than the mean stress factor due to its more significant variations, while the mean stress profile rather shows the stress concentration at the corner point, it remains everywhere else almost invariant.

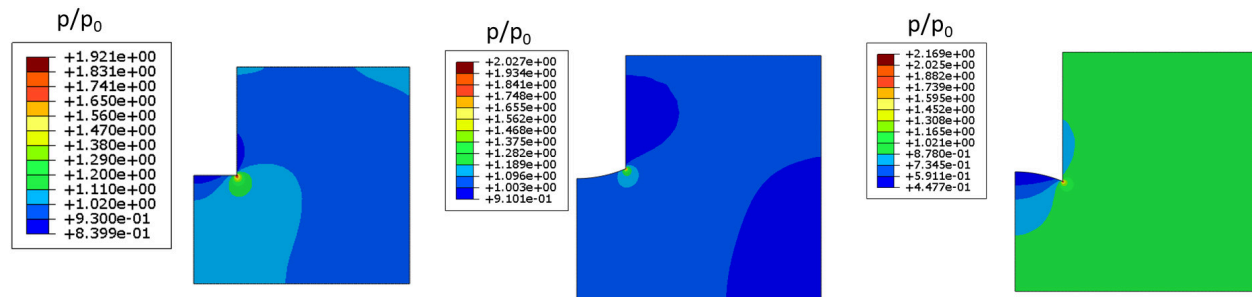


Figure 1: Mean pressure concentration factor for flat, convex, and concave profiles.

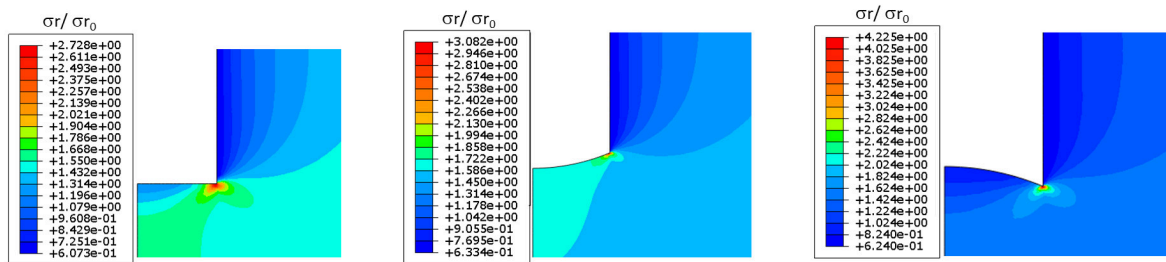


Figure 2: Radial stress concentration factor for flat, convex, and concave profiles.

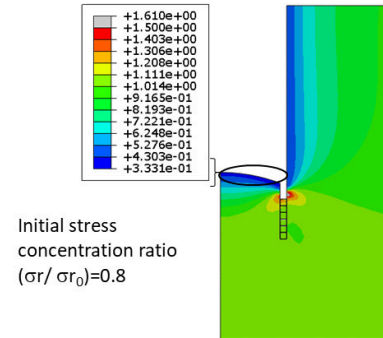
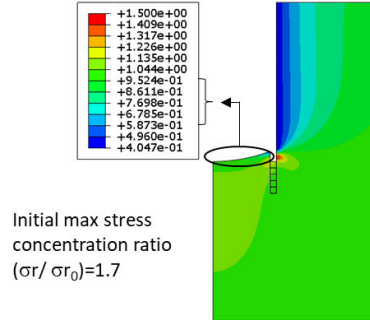
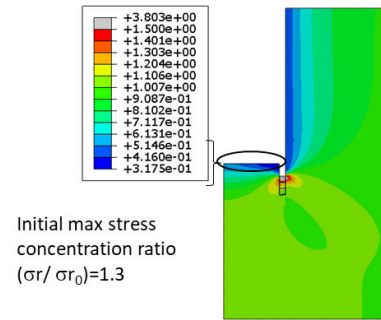
The stress can be concentrated at the bottom-hole depending on its profile (Figure 2). The curvature radius of the studied convex and concave profiles is $\pm 0.25\text{m}$. The convex profile results in a higher stress concentration rather at the centre of the bottom-hole whereas for the concave and flat profiles, this occurs more at the periphery of the bottom-hole. Interestingly, the concave profile exhibits stress relaxation except at the periphery of the hole.

2.3 How to release stress concentration ?

One of the major ideas of the ORCHYD project is to be able to release the bottom of the borehole, in the immediate vicinity of the action of the drilling tool, from the high stress concentrations deep hard rocks. This would reduce the resistance of these rocks to the cutting action and thus significantly improve the ROP. We have shown that one way to achieve this is to create a circular groove at the periphery of the drilled hole.

Numerical simulations show that the creation of such peripheral groove on the bottom-hole allows stresses to be released, this phenomenon is even more significant as the depth of the groove is greater. Figure 3 shows this fact for the studied profiles with a groove of 2 and 5 cm. For the flat profile, stress concentration factor decreases from a maximum initial value of 1.3 to almost 0.4-0.5 (~60%) when the groove depth is 2cm and could reached 0.25 (80%) with 5 cm groove. This trend is less significant for the convex profile for which with a groove depth of 2 cm the stress concentration factor changes from 1.7 to 0.75 (~40%) until 0.45 (~70%) with a groove depth of 5cm. The concave profile shows the lowest stresses concentration with or without the presence of the groove. Actually, the stress is already released by the concave profile itself before slotting the groove (~20%). A groove depth of 2cm further reduces the stress concentration factor (rather the relaxation ratio in this case) from 0.8 to 0.35 (~65%) up to 0.25 (~70%) with a groove depth of 5cm.

Groove depth =2cm



Groove depth =5cm

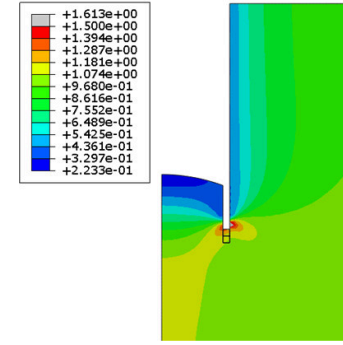
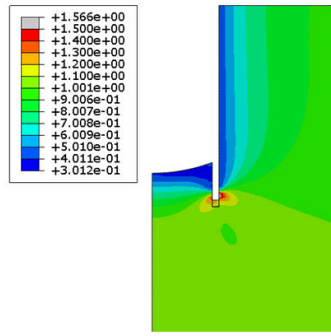
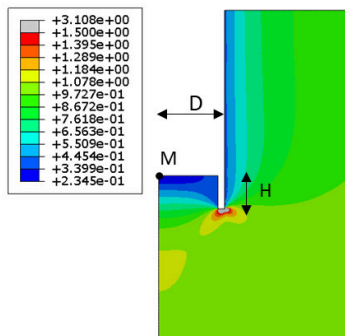


Figure 3: Stress release process for the studied profiles according to the groove depth.

The central point on the bottom-hole is the last point where the stress could be released by the peripheral grooving. That is why we choose this point (called M hereafter and depicted on figure 3) to analyse the potential optimization of the stress relaxation process in the next section.

Figure 4 shows a tensile zone in the case of concave profile, produced under an anisotropic stress condition ($\sigma_h = -100$ MPa and $\sigma_v = -150$ MPa). It is interesting to note that (only) concave profile gives rise to occurrence of tensile stress, and this could largely promote the cutting process because the rock within this zone is rather failed or not far from the tensile failure limit. This zone would present less resistance and should enhance the advancement of the drilling tool.

These results seem be similar to those obtained in several studies on core dinking process at great depth. All other things being equal, the difference of these two cases is the absence of mud pressure in core dinking phenomenon.

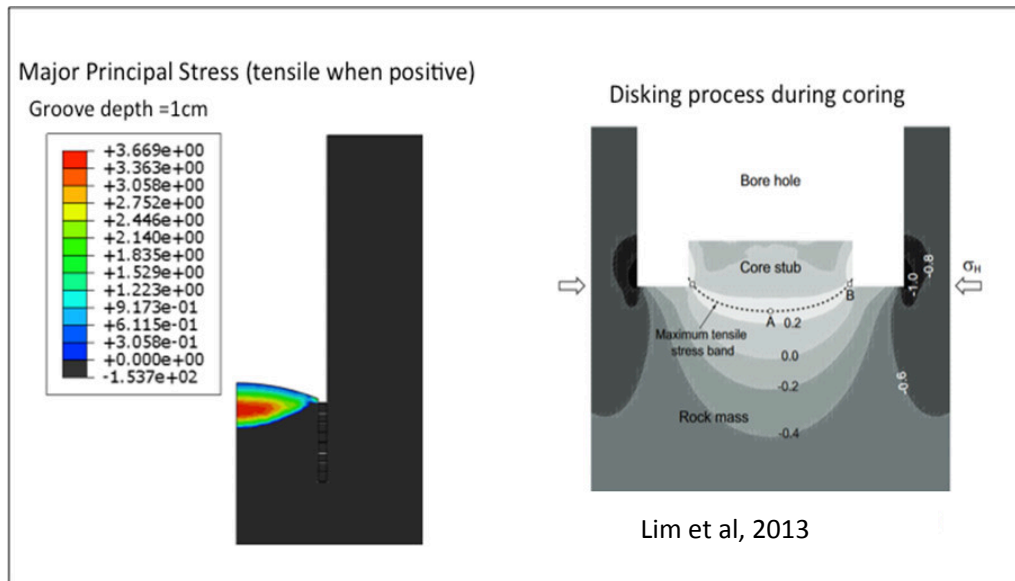


Figure 4: Tensile zone, -left) : concave profile with peripheral groove and -right) coring process according to Lim et al (2013).

3 Optimization of the stress release process

The simulations showed that using different bottom-hole profiles could result in different states of stress concentration/relaxation. This section deals with the optimisation of the release process by analysing the groove depth effect, while exploring the stress state and failure criterion for different bottom-hole profiles.

3.1 Effect of groove depth

To synthesize the groove depth effect, we introduced a dimensionless parameter $\eta=H/D$, where H is the groove depth and D the bottom-hole radius. The radial stress concentration factor evolution at point M is presented in Figure 5 as function of η parameter. As discussed earlier, the convex profile could generate a stress concentration at the bottom-hole centre, before starting the slotting process, that is why the blue line starts with a value higher than 1. On the contrary, the concave profile starts with a radial stress factor of 0.62. The same tendency is shown on Figure 6 when considering the mean stress.

It can be seen from figure 5 and 6, that for flat and concave profiles, to reduce the radial stresses (or mean stresses) at the centre of the bottom-hole by more than 50%, the depth of the peripheral groove must be 20 to 30% the hole radius. To achieve the same rate of relaxation with a convex profile, the depth of the peripheral groove should go further than 50% of the hole radius.

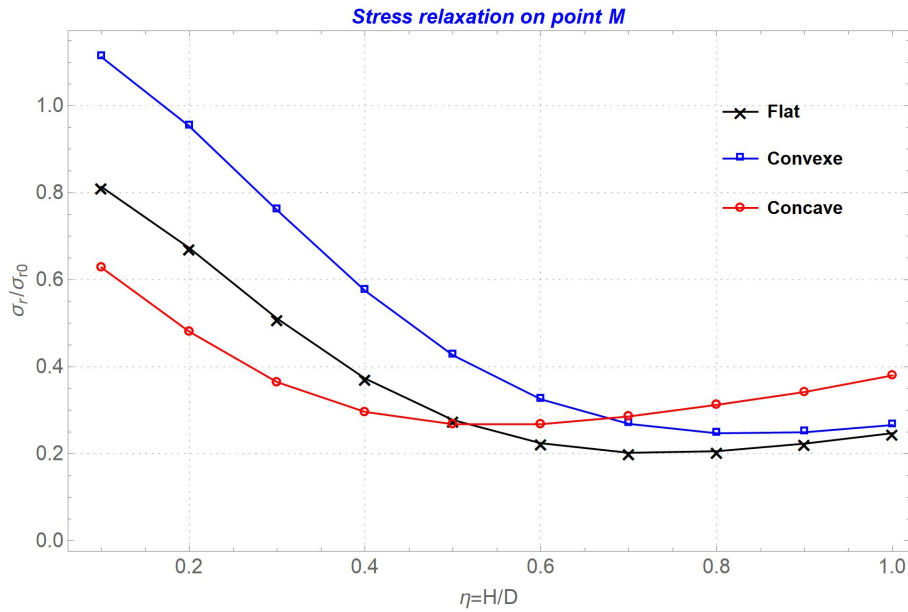


Figure 5: Stress release using radial stress concentration factor

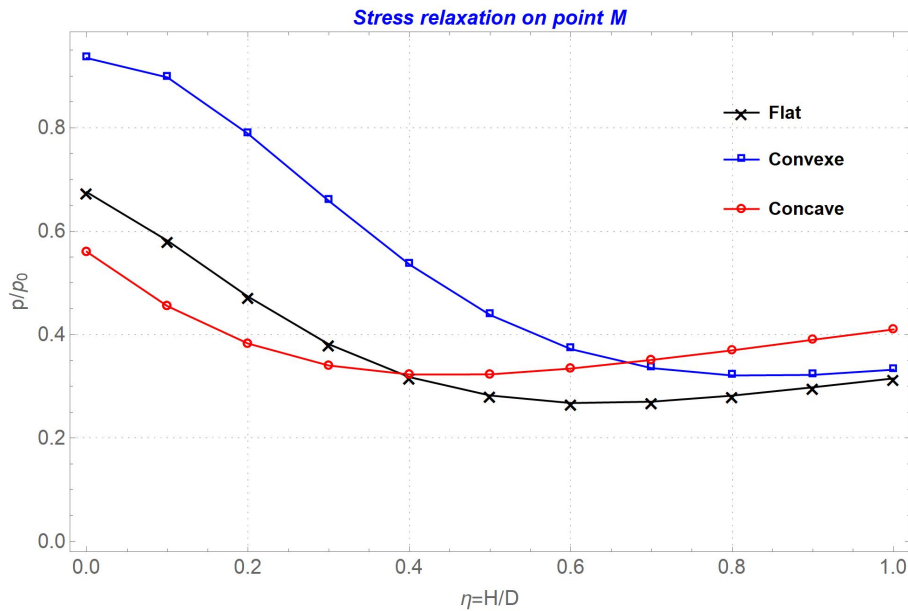


Figure 6: Stress release using mean stress concentration factor

It can also be seen in these figures that there is an optimum groove depth for each profile. In addition, these results demonstrate the interest of concave profile and promote using concave drilling bit in particular for the range of shallow groove depth. This finding will be investigated in the next section using a failure criterion.

3.2 Failure criteria

In this section we will analyse the relative stress state of each bottom-hole profiles and compare them to different failure criteria in order to assess the more effective profile that could yield the larger plastic or damaged area into the rock. This will be done via a post-processing analysis on the elastic simulations results. Different failure criteria are used classically in the literature. The Mohr-Coulomb and the Drucker-Prager are the most used ones, but they seem to be reliable for moderately stressed rocks. At high pressures (the case of deep drilling),

strength becomes insensitive to pressure and rock failure envelope gets a concave shape toward the mean stress (Lockner, 1995). Literature review shows also that these criteria do not properly account for the tensile failure limit (Pouya et al, 2017). To clarify these purposes, in addition to the two above-mentioned failure criteria, we will also use a modified Hoek and Brown criterion.

In order to compare these failure criteria, we will present them in the p-q plan (pressure – deviator stress) where $p = -\frac{tr(\underline{\underline{\sigma}})}{3}$, $q = \sqrt{\frac{3}{2} \underline{\underline{s}} : \underline{\underline{s}}}$ and s denotes the deviatoric part of the stress tensor: $\underline{\underline{s}} = \underline{\underline{\sigma}} + p\underline{\underline{I}}$ (I stands for Identity tensor). The third stress invariant stands for the Lode angle is defined as $\theta = \arccos\left(\frac{3s_1}{2q}\right)$ and will be fixed to zero in this study for the sake of simplicity. The objective is to write all these criteria in the general form of $F(p,q, \theta)=q-g(\theta)f(p)=0$. The reason for this transformation is to be able to take into account the effect of the mean stress in our simulations using different failure criteria. The stress transformation is given in Rouabhi (2004), herein we present the final form of each criterion in p-q plan.

$$\text{Mohr-coulomb : } F(p, q, \theta) = q - g(\theta)f(p) = 0 \quad (1)$$

$$\text{With } g(\theta) = \frac{1}{A_k \cos \theta + \sin\left(\theta + \frac{\pi}{6}\right)}$$

$$\text{fixing } \theta = 0 \text{ as mentioned, it becomes } g(\theta) = \frac{2}{1+2A_k}$$

$$f(p) = \frac{3}{2}[R_c + (A_k - 1)p] \quad (2)$$

A_k and R_c are the model parameters in relation with the friction angle (ϕ) and the cohesion (c):

$$A_k = \frac{1+\sin \phi}{1-\sin \phi} \text{ and } R_c = \frac{2c}{1-\sin \phi} \text{ that stands for the uniaxial compression strength.}$$

$$\text{Drucker-Prager : } F(p, q, \theta) = q - f(p) = 0 \quad (3)$$

With $f(p) = \alpha_1 p + \alpha_2$ where α_1 et α_2 are material parameters and for $\theta = 0$ case they can be described as following: $\alpha_1 = \frac{6\sin(\phi)}{3+\sin(\phi)}$ and $\alpha_2 = \frac{6c\cos(\phi)}{3+\sin(\phi)}$. It can be noticed that for $\alpha_1=0$ one can obtain the Von Mises's criterion.

$$\text{Hoek and Brown : } F(\bar{p}, \bar{q}, \theta) = \bar{q} - l(\theta)f(\bar{p})$$

$$f(\bar{p}) = -\frac{m}{6} + \frac{1}{2}\sqrt{\frac{m^2}{9} + 4(m\bar{p} + c)} \quad (4)$$

Where m , c and R_c are material parameters (same as Mohr-Coulomb model) and for parameter m the following approximation is common: $\frac{R_T}{R_c} \approx \frac{1}{m}$. R_T stands for the tensile strength.

$\bar{p} = \frac{p}{R_c}$, $\bar{q} = \frac{q}{R_c}$ and $l(\theta) = 1$ in our case. To present more non-linearity of this failure criterion, we propose a general formulation by adding a power law on function of $f(\bar{p})$. The final criterion becomes as presented by equation 5. For $n=1$ we have the classical Hoek and Brown criterion.

$$F(\bar{p}, \bar{q}) = \bar{q} - f(\bar{p})^n \tag{5}$$

Figure 7 summarizes all the studied criteria using the same parameters depicted on table 1.

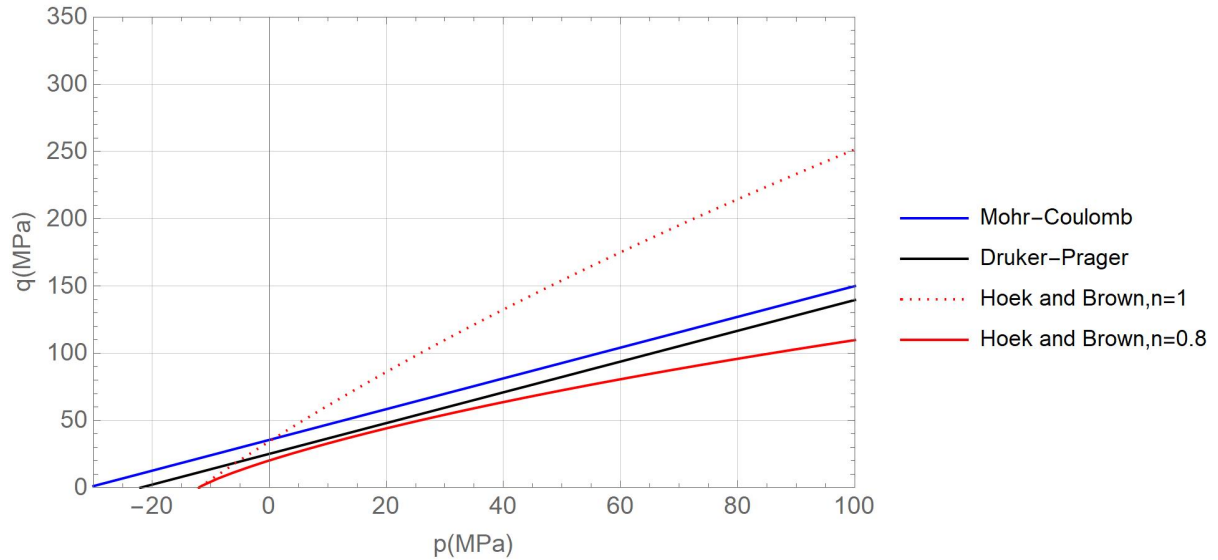


Figure 7: Studied failure criteria.

The classical HB (Hoek and Brown) overestimated the shear strength while with an $n=0.8$, it becomes as close as possible to two other models and will be used thereafter. As it was mentioned, Mohr-Coulomb (MC) and Drucker-Prager (DP) over-estimate the tensile strength as well as the shear strength for the high value of pressure. Three studied profiles (concave, convex and Flat) will be passed under review of the stress state analysis via the presented criteria. It can be expected that the HB criterion gives the more critical results in terms of plastic zone.

Figure 8 shows the stress state of the bottom-hole of flat profile after cutting a 1 cm groove depth.

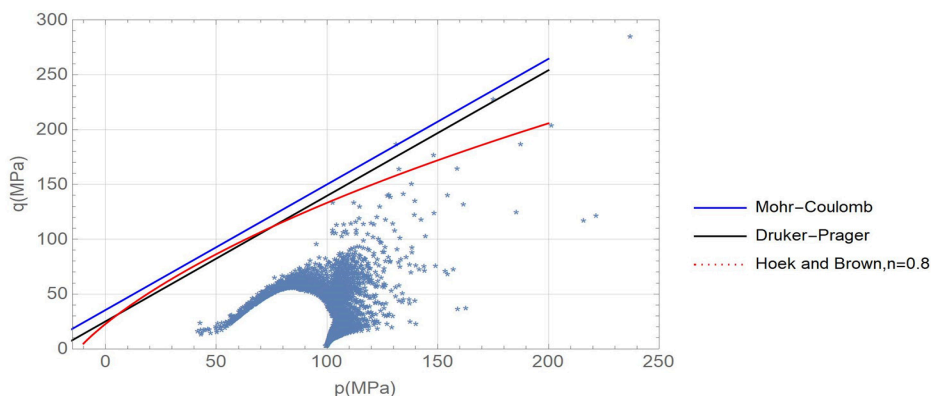


Figure 8: Stress state around flat profile bottom-hole with a 1 cm groove depth.

As can be observed on figure 9, the points corresponding to the stress state of the concave profile (blue points) are closest to the HB failure criterion or even have exceeded it. That means

the concave profile contributes more to the weakening of the bottom-hole. One can observe that any tensile failure happens after slotting a groove of 1cm depth under isotropic condition.

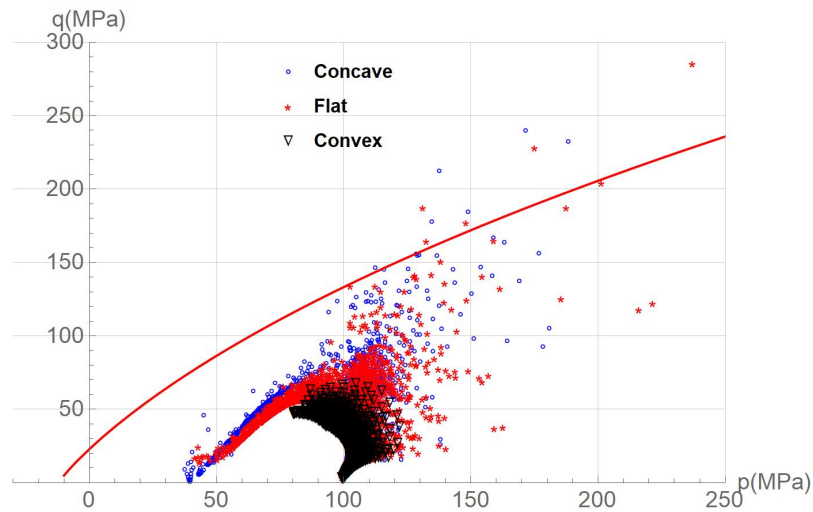


Figure 9: Stress state at the bottom-hole with 1cm groove depth for the three profiles.

To gain some insight into the stress path, we can study the principal stress history of a point in the centre of the bottom-hole (point M) with and without grooving. Figure 10 shows this fact for these two cases using a flat profile.

Figure 10 shows the path of the maximum principal stress for point M from its initial position 10 cm below the bottom of the hole, to the final position where it reaches the rock free surface (subject to mud pressure). The stress starts by an isotropic state ($s_1=s_3=-100$ MPa) and finishes on a state corresponding to ($s_1=-40$ MPa and $s_3=-85$ MPa) for the case without groove. Whereas, with a 2 cm groove, the final state can reach a more relaxed radial stress condition ($s_3=-52$ MPa, blue curve).

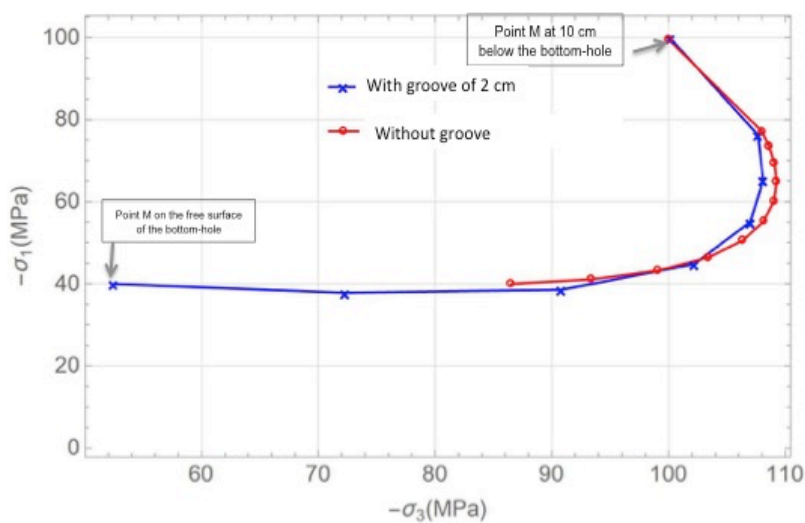


Figure 10: Stress path for point M in the centre of the bottom-hole surface, with and without groove of 2 cm depth.

In a diagram mean stress-deviatoric stress, the same stress path is shown in figure 11 which show that the final stress state with a groove has less deviator and less mean stress than without groove. This should correspond to more favourable drilling conditions.

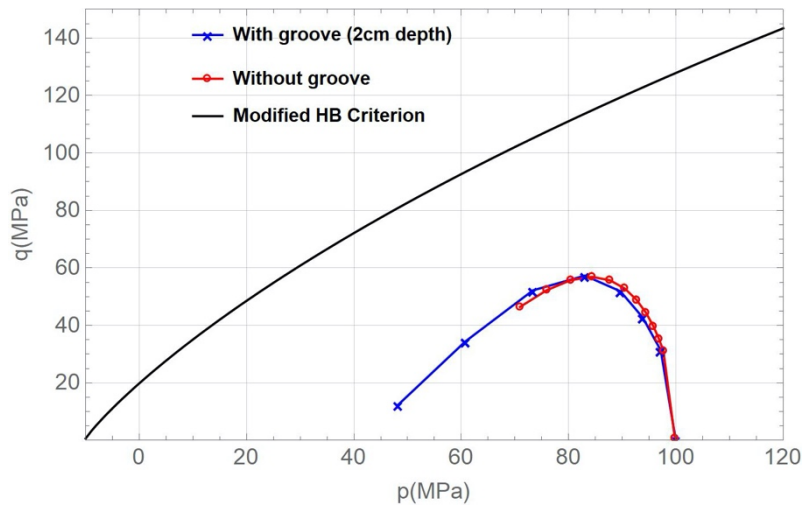


Figure 11: Stress path in the diagram mean stress-deviator at point M, centre of bottom-hole surface, with and without groove of 2 cm depth.

Before concluding this section, we can analyze the elastic strain energy. It should be noted that the dissipated “plastic” energy is more consistent term to analyze the energy release during a thermo-mechanical process. Figure 12 shows the effect of the groove depth on the elastic strain energy and confirms the more beneficial effect of the concave profile. It should be noted that this figure corresponds to the point M at the centre of the bottom-hole and agrees well with the previous discussions. It can be observed from this figure that a groove depth beyond 3-4 cm has no effect for concave and flat profiles, while it can still release the energy for the convex profiles.

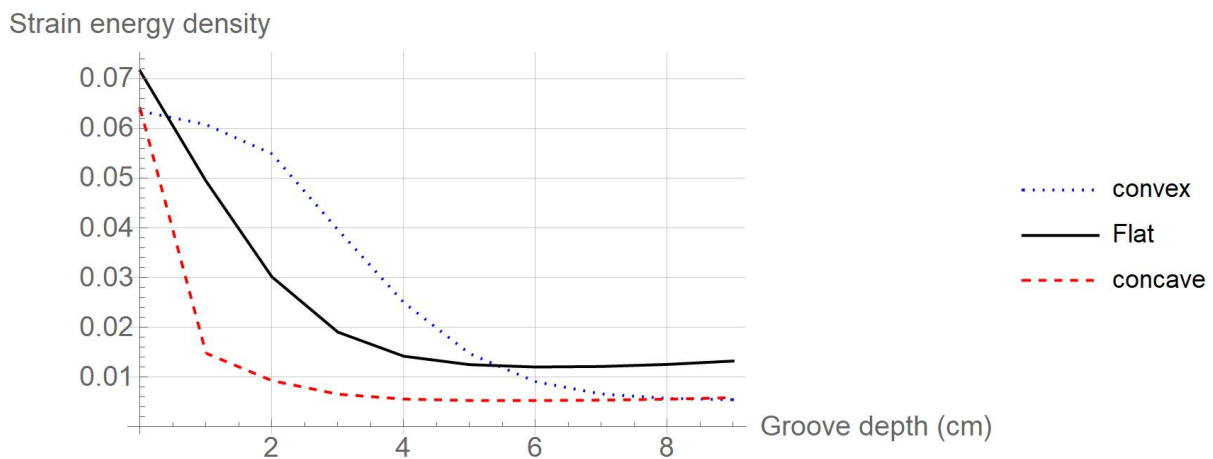


Figure 12: The groove depth effect on the elastic strain energy density for the studied profiles.

This section results have highlighted the efficiency of the concave profile in stress release process comparing to two other studied profiles where the flat and convex profiles show intermediate and low potential respectively.

4 Can these processes be reproduced under laboratory conditions?

The principle of stress concentration and its release when slotting peripheral grooves on the bottom-hole should be proven using controlled pilot tests on the ARMINES drilling bench.

In this context, can bottom-hole stress concentration and relaxation processes be reproduced during laboratory drilling and what impact would they have on the ROP, and how can the tests be designed to demonstrate these processes?

Figure 13-a schematically illustrates the conditions of the laboratory drilling test in terms of rock sample dimensions, geostatic stresses and drilling fluid pressure imposed to the rock sample to be drilled. Figure 13-b shows an example of numerical results for a flat profile, which is intermediate in terms of stress concentration between convex and concave profiles. This is the distribution of the radial stress concentration factor along the borehole radius, with and without the presence of a peripheral groove, in the case of a full-scale borehole and a laboratory-simulated borehole under the same conditions (rock, borehole diameter, geostatic stresses, drilling fluid pressure, depth of the peripheral groove). It is noted that the surface borehole has slightly higher stress concentration factor in the laboratory test case than in the real (in-situ) case. However, the levels remain comparable in both cases.

Furthermore, the creation of a peripheral groove seems inducing the same level of stress relaxation between the real and the laboratory cases.

These simulations show that the laboratory test produces results close to those obtained numerically at the scale of a real borehole. In all cases, it does not amplify the stress concentration and relaxation processes compared to the real case.

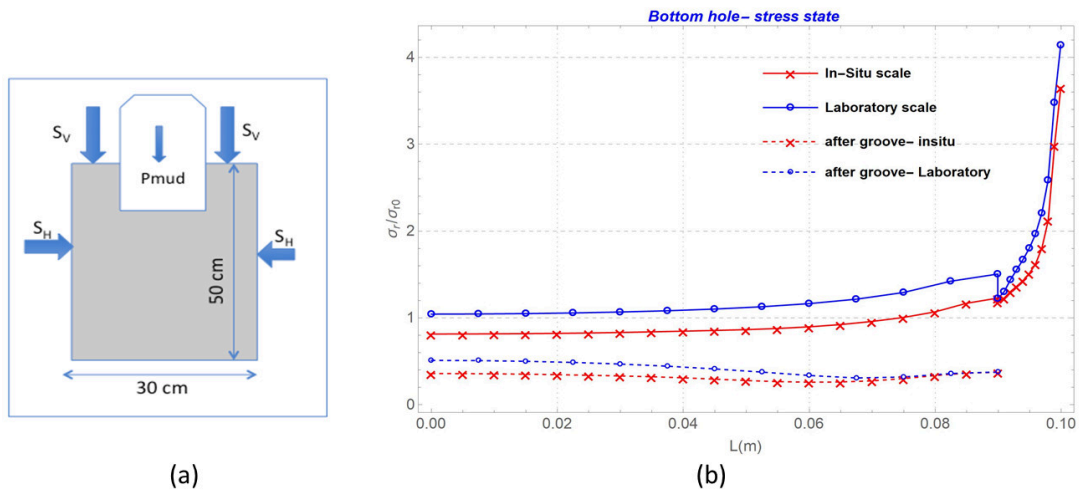


Figure 13 : a) laboratory test scheme , b)radial stress concentration factor, in-situ and laboratory scales, along the radial distance L on the bottom-hole surface (20 cm hole diameter).

Figure 14 shows the difference between these two configurations concerning the effect of groove depth on radial stress release rate.

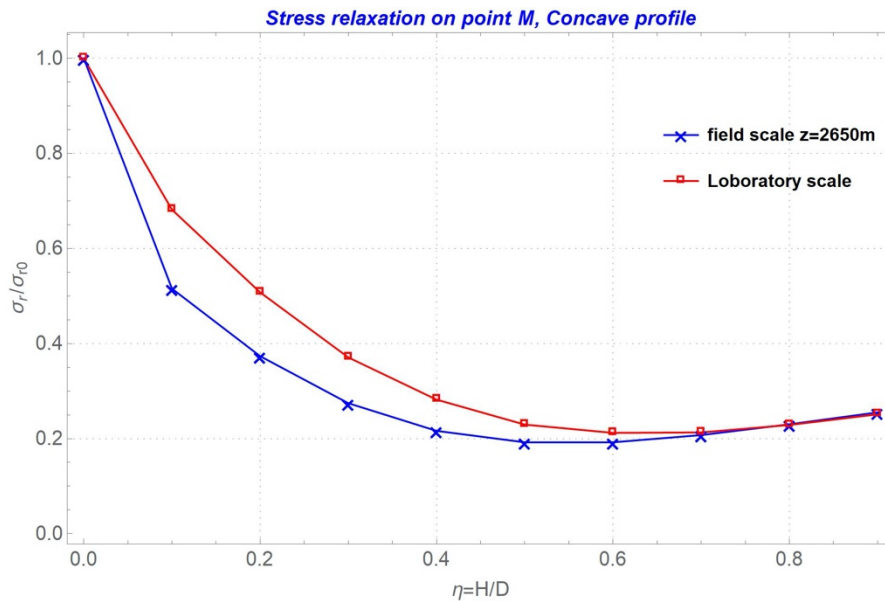


Figure.14: Radial stress release for the field scale and laboratory scale configurations.

The first laboratory condition that could potentially affect the modelling pattern is the applied mud pressure that will be different from the initial stress (due to test complexity). Before studying the effect of a peripheral groove on the ROP, it is necessary to reproduce the phenomenon of stress concentration at the bottom-hole due to the disturbance of the initial stress field.

The mud pressure was fixed to 25.5 MPa and the initial stress to 70 MPa in laboratory scale (corresponding to the 2560 m of depth with granite and to the upper limit of the drilling bench). The rock sample under these initial conditions would undergo a non-hydrostatic boundary stress generating potentially significant shear stress before the drilling process starts. To overcome this problem, we first calculate a distance from the top surface of the rock sample that was not yet been affected by the drilling process. This distance is almost 12 cm whereupon the mean stress is almost constant. In the second step we drill this thickness of 12 cm under a constant mud pressure. Afterward we drill 10 cm without creating groove and then 10 cm with groove creation to study its contribution to ROP. We drill a second section of 10 cm in combined mode (drilling+groove slotting) to study the contribution of the groove to the ROP.

5 General conclusions

This report summarizes the results of the numerical simulations subject of task1 of WP4, intended to provide a preliminary design of the geometry of the bottom-hole and the groove to be slotted on the bottom-hole in order to release stresses in the context of deep drilling in hard rocks such as granites.

These simulations were performed in the framework of an axisymmetric elastic model for three bottom-hole profiles: flat, convex and concave. These profiles were found to be key factors that can be played on to optimize the drilling process.

Whatever the profile of the bottom-hole, to reduce (by more than 50%) the radial (or mean) stress, at the immediate vicinity of the drilling bit action, the depth of the peripheral groove must reach 20 to 30% the hole radius. The concave profile shows a relaxation process in the centre of the hole without the presence of the peripheral groove. The creation of the groove also induces relatively the same effect as in the case of other profiles, which demonstrates the interest of this type of profile and therefore the use of a concave bit.

Furthermore, these simulations show that the laboratory test produces results close to those obtained numerically at the scale of a real borehole. In all cases, it does not amplify the stress concentration and relaxation processes compared to the real case.

6 Discussions and perspectives

6.1 Initial stress state and limit of axisymmetric simulations

In this study we have analysed an isotropic initial state as well as a plan anisotropic condition ($s_h = -100$ MPa and $s_v = -150$ MPa) for which only the concave profile gave rise to a tensile failure occurrence (figure 4). Stress anisotropy factor is more relevant in a 3D analysis where two lateral stresses could be different ($s_{yy} \neq s_{xx}$).

Some authors have highlighted the influence of anisotropy of two horizontal principal stresses on the formation of the core disking phenomenon (Wu et al, 2018).

The limit of an axisymmetric simulation is to take into account properly this 3D stress anisotropy. Figures 15 and 16 show the stress state of bottom-hole considering the initial stress anisotropy without and with the mud pressure respectively. Figure 15-b shows that the disking phenomenon is more likely to occur under stress anisotropy condition.

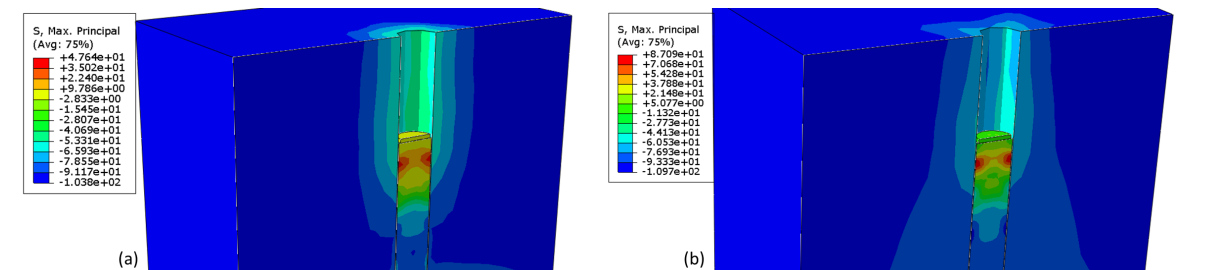


Figure 15: Anisotropy effect without mud pressure on principal stress [MPa] a) isotropic condition ($s_{xx} = s_{yy} = s_{zz}$), b) anisotropic condition ($s_{xx} = 2s_{yy} = 2s_{zz}$).

The Figure 16-a shows the major principal stress under isotropic stress condition when a groove of 1cm is slotted. The major principal stress remains compressive all over the rock. Figure 16-b shows the same simulation when an anisotropic initial stress condition is considered. The major principal stress could pass to tensile throughout the peripheral part of the borehole. These anisotropy analyses could not be pointed out within an axisymmetric simulation. This means that the conclusions drawn from the axisymmetric simulations are less favourable in terms of rock weakening and therefore in terms of deep rock drillability.

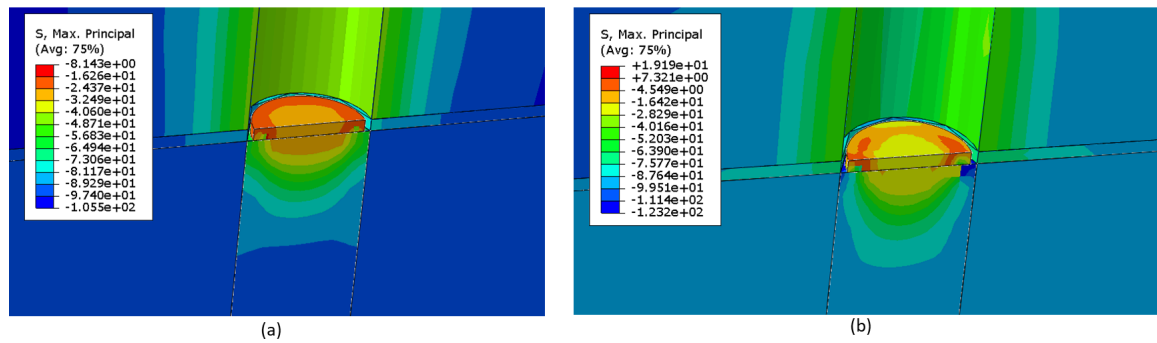


Figure 16: Anisotropy effect, groove depth of 1cm, a) principal stress [MPa] under isotropic condition ($s_{xx} = s_{yy} = s_{zz}$), b) principal stress under anisotropic condition ($s_{xx} = 2s_{yy} = 2s_{zz}$).

6.2 Thermal effect

It would be interesting to study the combined effect of high temperature and stress concentration on rock strength and failure.

Using a temperature dependent failure criterion, the shear strength could be weakened (Tien et al, 2013), and the shear failure could occur at the bottom-hole by stress concentration. Figure 17 shows this effect when the MC failure criterion (eq.1) is used and the cohesion is degraded by temperature. This figure shows the bottom-hole's new stress distribution when the difference of temperature between the rock mass and the mud is considered. The temperature has a dual effect on the rock behaviour. The difference of temperature between the mud and the rock mass could induce tensile stress and could simultaneously reduce the rock strength (Gautam et al, 2018). The maximum principal stress increases by increasing temperature gradient, which is beneficial to rock fragmentation.

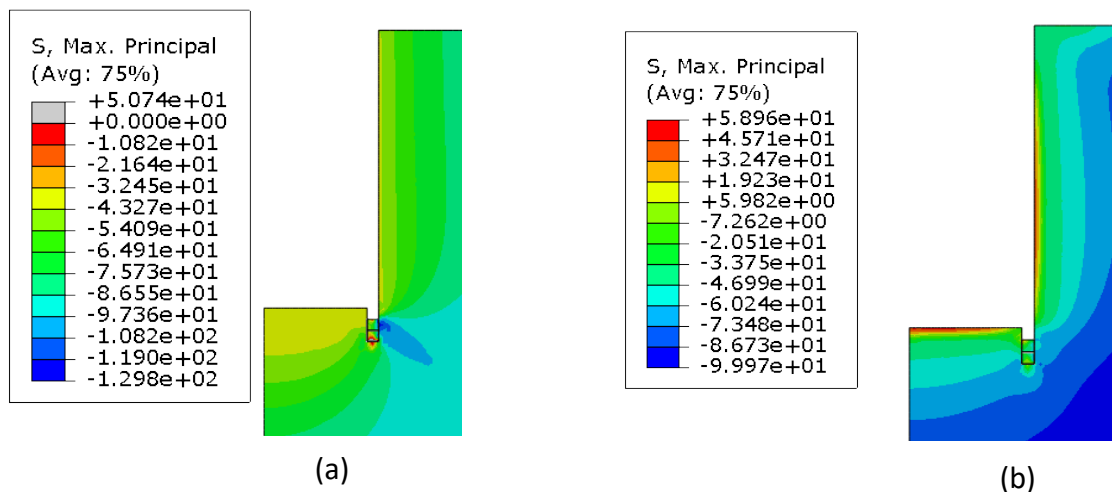


Figure 17: a) maximum principal stress (MPa) without temperature variation, b) maximum principal stress with temperature variation (mud injected temperature 60 °C, rock initial temperature 200 °C).

7 References

- Bahrani, N., Valley B., Kaiser P.K. (2015). Numerical simulation of drilling-induced core damage and its influence on mechanical properties of rocks under unconfined condition. *International Journal of Rock MEchanics and Mining Sciences*, 80, 40-50
- Gautam P.K., Verma A.K., JHA M.K., Sharma P., Singh T.N. (2018). Effect of high temperature on physical and mechanical properties of Jalore granite. *Journal of applied Geophysics*, Volume 159, 460-474.
- Lim S.S., Martin C.D, Christensen R. (2013); Core diskings observations and in-situ stress magnitude. American Rock Mechanics Association.
- Lockner D.A. (1995). Rock failure. Book, Published by American Geophysical union.
- Pouya A., Nguyen M.T. and Tang A.M. (2017). Un crière hyperbolique simple de resistance des roches. *Rev. Fr. Geotech.* 152, 3.
- Rouabhi A. (2004). Dynamic behaviour and fragmentation of quasi-brittle materials, Application to rock fragmentation by blasting. PhD thesis of école des Mines de Paris. Tian H., Kempka T., Xu N., Ziehler M. (2013). A modified Mohr-Coulomb Failure Criterion for Intact Granites Exposed to high temperatures. *Clean Energy System in the subsurface*. Springer series in Geomechanics and Geoengineering.
- Wu S., Wu H., Kemeny J., (2018). Three-dimensional discret element method simulation of core diskings. *Acta Geophysica*, 66, 267-282.